AIChE

Experimental and Theoretical Study of Methane Adsorption on Granular Activated Carbons

Yuguo Wang, Cemal Ercan, Anwar Khawajah, and Rashid Othman
Research & Development Center, Saudi Arabia Oil Co., Dhahran, 31311, Saudi Arabia

DOI 10.1002/aic.12611
Published online April 27, 2011 in Wiley Online Library (wileyonlinelibrary.com).

The experimental and theoretical study of methane adsorption on granular activated carbons is presented. The adsorption data are modeled by various isotherm equations. Toth equation is found to have the best fit. The isosteric heat decreases with loading and increases weakly with temperature, which is an indication of heterogeneity of the methane and granular activated carbon system. Using optimized parameters from Toth equation, a novel procedure is developed to calculate the integral heat of adsorption, which is the total amount of isosteric heat of adsorption at a given temperature and pressure during the adsorption process. © 2011 American Institute of Chemical Engineers *AIChE J,* 58: 782–788, 2012

Keywords: methane adsorption, Toth equation, activated carbon, isosteric heat, integral heat of adsorption

Introduction

Depending on the source and geographical location of production, natural gas can contain up to 95 mol % methane (CH_4), the remaining being carbon dioxide (CO_2), nitrogen, and small amounts of higher molecular weight hydrocarbons, such as ethane (C_2H_6), propane (C_3H_8), and butane (C_4H_{10}). It is well-known that natural gas burns cleaner than gasoline, diesel and the other fuels. Because of this environmentally friendly behavior, it is commonly used for heating and its use continues to grow. It is also used in some vehicles by storing it as compressed natural gas (CNG) at pressures up to 270 atm. In current practice, natural gas is mainly stored as CNG for vehicle use or liquefied natural gas (LNG) for shipment. However, CNG requires expensive vessels and multistage compression and LNG also requires expensive cryogenic process. An attractive alternative to CNG and LNG might be adsorbed natural gas (ANG), where the gas is stored on porous material packed into a vessel at much lower pressure. ANG uses microporous adsorbents inside a vessel, which offers higher energy density and higher volume to volume (v/v) storage capacity compared with CNG at typical natural gas pipeline conditions, pressure less than 50 bars and temperature less than 55°C.[1–9] So, at these conditions, ANG has high potential for exploitation not only in transportation but also in large-scale application such as ANG storage close to natural gas consumers.

In ANG operation, the most important is the selection or development of a microporous material with high-storage capacity and stability under cyclic operation. Potential microporous materials, which can meet these requirements, include activated carbon, metal-organic frameworks (MOF), and other organic or inorganic solids.[10–20] Although MOFs and the other organic solids display attractive sorption properties with a v/v adsorption capacity as high as 230 of absolute methane adsorption at 290 K and 35 bar, which also exceeds the DOE target of 180 v/v, methane is strongly entrapped in MOF's structures and heating up to 100°C is necessary for desorption.[13] The other factors, which may also affect the applicability of MOFs as natural gas adsorbent include their stability and ability to tolerate impurities such as H_2S, black powder, mercaptans, etc., which are

Correspondence concerning this article should be addressed to C. Ercan at cemal.ercan@aramco.com.

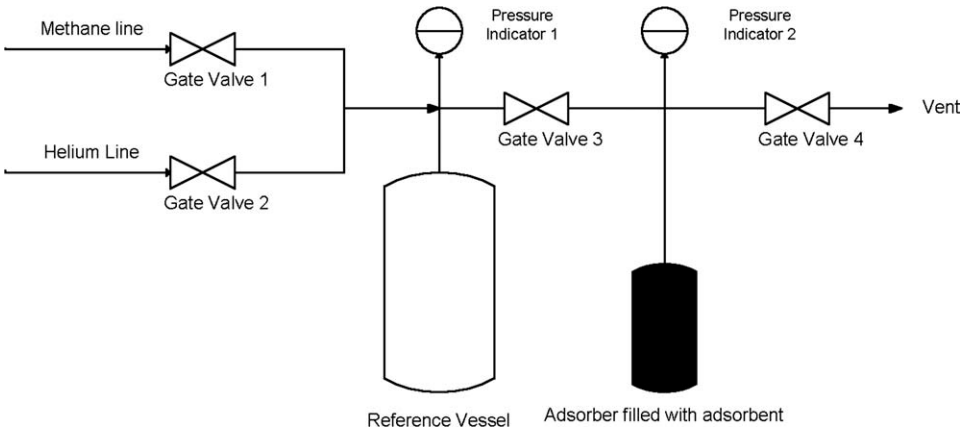

Figure 1. Schematic diagram of the experimental setup.

common in industrial applications. Inorganic solids like zeolites have lower performance for methane storage than activated carbons. Moreover, zeolites present much more hydrophilic surfaces than carbons and tend to adsorb water preferentially. Therefore, activated carbon currently remains the only commercially viable adsorbent for natural gas storage in terms of adsorption capacity and stability.

In this article, both experimental and theoretical investigations were carried out to determine the methane adsorption capacity of various granular activated carbons under temperature range up to 56°C. Temperature-dependent Sips, Toth and Unilan isotherm equations were used to fit the adsorption data. D-A equation was used to optimize parameters for adsorption characteristic curve. A novel procedure is also developed to predict the total amount of isosteric heat of adsorption process.

Experimental

Experimental setup and procedure

In this study, the volumetric method was used to measure the methane adsorption on granular activated carbons. The major components of the experimental setup are shown in Figure 1. A vacuum pump, not shown in Figure 1, is also connected to the system for degassing. The adsorber has a thermal jacket connected to a heater/chiller so that the temperature of the adsorber can be set to the desired temperature for measurement.

To determine the adsorption isotherm, the adsorber was first filled up with 50 g of granular activated carbon and was degassed at a pressure of 2.5×10^{-4} Torr at 120°C for 4 h. Then, the adsorber was cooled down to and maintained at desired temperatures of 10, 21, 38 or 56°C. The reference vessel has a volume of two liters, and the adsorber has a volume of 120 cm^3. The reference vessel was first charged with methane to a certain pressure, then, valve 3 was opened and the pressure between two vessels was left to equalize. Readings of the two pressure indicators were taken after 20 min of reaching equilibrium.

Materials

Four types of commercial granular activated carbons, labeled as AC1, AC2, AC3 and AC4, with different physical characteristics were used. The high-purity methane and ultra-high-purity helium were used without further purification.

Characterization of activated carbons

Micromeritics ASAP surface area and porosity analyzer were used for N_2 adsorption/desorption at 77 K. The physical properties measured are in Table 1. Here, the total pore volume from nitrogen porosimeter is for the pores that have a diameter range of 0–20 nm, and the micropores are defined as the pores that have diameters range of 0–2 nm. For the mercury porosimeter, mesopore volume is for pores with a width range of 2–50 nm, and macropores are pores with a width range of 50–10,000 nm.

The amount N_2 adsorbed vs. relative pressure at 77 K on granular activated carbons are shown in Figure 2. The shapes of these four isotherms are Type-II isotherm, which indicates that these granular activated carbons are essentially microporous. After the relative pressure of 0.8, the increase of adsorbed amount is most probably due to the presence of mesopores, where the condensation of N_2 occurs as the pressure goes up. It is also noted that the isotherm plateau is reached at P/P0 = 0.5. The slope of the plateau is related to the multilayer mechanism of adsorption on the external surface of the materials. It is also obvious that the higher surface a granular activated carbon has, the higher mass to mass (m/m) adsorption capacity it has for nitrogen.

Table 1. Physical Properties of the Granular Activated Carbon Samples

Sample	AC1	AC2	AC3	AC4
ASTM mesh size	8×16	30×70	2×60	12×40
Bulk density (g/cm^3)	0.47	0.39	0.49	0.54
Skeletal density (g/cm^3)	2.299	2.363	2.402	2.059
Nitrogen Porosimetry (77 K)				
BET surface area (m^2/g)	1235	1589	1426	999
Total Pore Volume (cm^3/g)	0.629	0.747	0.599	0.500
Micropore Volume (cm^3/g)	0.600	0.706	0.560	0.456
BJH average pore width (Å)	18.00	18.70	17.47	20.64
Mercury Porosimetry				
Total pore volume (cm^3/g)	0.388	0.457	0.360	0.314
Mesopore Volume (cm^3/g)	0.182	0.205	0.164	0.137
Macropore Volume (cm^3/g)	0.205	0.252	0.194	0.176

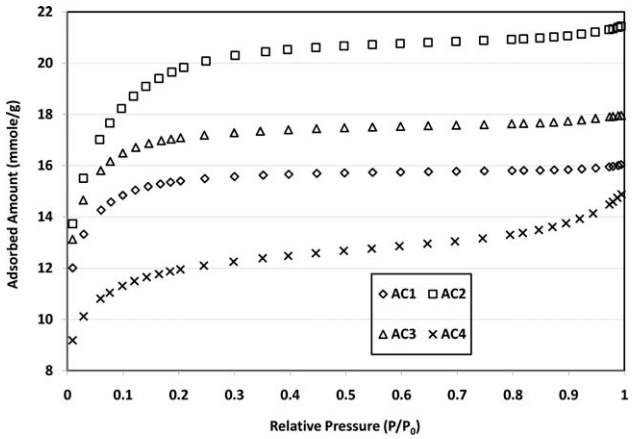

Figure 2. N_2 adsorption isotherms at 77 K on granular activated carbons.

Determination of adsorption of methane

After the adsorber was filled with granular activated carbon, it was tapped gently until the level of the granular activated carbon did not go down anymore. At this point, the granular activated carbon was packed to its bulk density. The total volume of the adsorber cell (V_{absorber}) consists of the following volumes: adsorbent skeletal (V_{sk}), micropore (V_{mic}), mesopore (V_{mes}) and macropore (V_{mac}), and the space among the adsorbent particles (V_{interp}). For precise determination of the total volume of micropore, mesopore, macropore of the adsorbent and the space among adsorbent particles, helium was used since it is essentially inert for adsorption. To determine the adsorption amount, pressure P_1 was recorded for the reference cell with a volume of V_{ref}, and equilibrium pressure P_2 was also recorded after the gate valve 3 was open. Then, the total volume becomes ($V_T = V_{\text{ref}} + V_{\text{absorber}}$). The nonskeletal volume is defined as

$$V_{nsk} = V_T - V_{sk} \tag{1}$$

Assuming that the methane adsorption only takes place in micropores, methane molecules inside the mesopore and macropores behave like in gas state. Gas-phase methane volume is, therefore ($V_{\text{nsk}} - V_{\text{mic}}$). To calculate the amount of methane adsorbed per gram of granular activated carbon, nonideal behavior is considered and Eq. 2 is used. This volumetric measurement of adsorption is similar to the methods applied by Gummar and Talu[21] and Salehi et al[22]

$$n_{adsorbed} = \frac{\left[\frac{P_1 V_T}{ZRT} - \frac{P_2 \times (V_{nsk} - V_{mic})}{ZRT}\right]}{M_{gac}} \tag{2}$$

where Z is methane compressibility factor, T is temperature, and R is the ideal gas M_{gac} is the mass of the granular activated carbon used. Z is determined from the well-known Soave-Redlich-Kwong (SRK) equation of state.

Results and Discussion

Experimental results

Figure 3a and 3b show the plots of the amount of adsorbed methane vs. pressure at 21°C for the four different granular activated carbons. All of them have Type-I isotherm, which indicates that the materials are microporous. Based on the moles of methane adsorbed per gram of granular activated carbon in Figure 3b, the capacity for methane adsorption for four granular activated carbons increase in the order of AC4 < AC1 < AC3 < AC2. This order is the same as the order of BET surface area of AC4(999 m^2/g) < AC1(1235 m^2/g) < AC3(1426 m^2/g) = AC2(1589 m^2/g). This is consistent with the order of the amount of N_2 adsorbed at 77 K on these samples as in Figure 2. The higher-surface area a granular activated carbon has the more moles of adsorbate it adsorbs. Based on the volume of methane adsorbed per bulk volume of granular activated carbon in Figure 3a, the capacity for methane adsorption increases in the order of AC4 < AC2 < AC1 < AC3. This capacity for methane adsorption change can be attributed to the fact that bulk density in volume to volume comparison becomes a more important factor. The bulk density for the four granular activated carbons are AC1(0.47 g/cm^3), AC2(0.39 g/cm^3), AC3(0.49 g/cm^3) and AC4(0.54 g/cm^3). Although AC2 has the largest BET surface area, it has the lowest bulk density. Then, for the same volume, AC2 will have the lowest mass packed. AC3 has the second highest BET surface area and bulk density, and AC4 has the highest bulk density, but lowest BET surface area. Therefore, it is reasonable to say that the synergetic effect between BET surface area and bulk density makes AC3 have the highest volume to volume adsorption capacity.

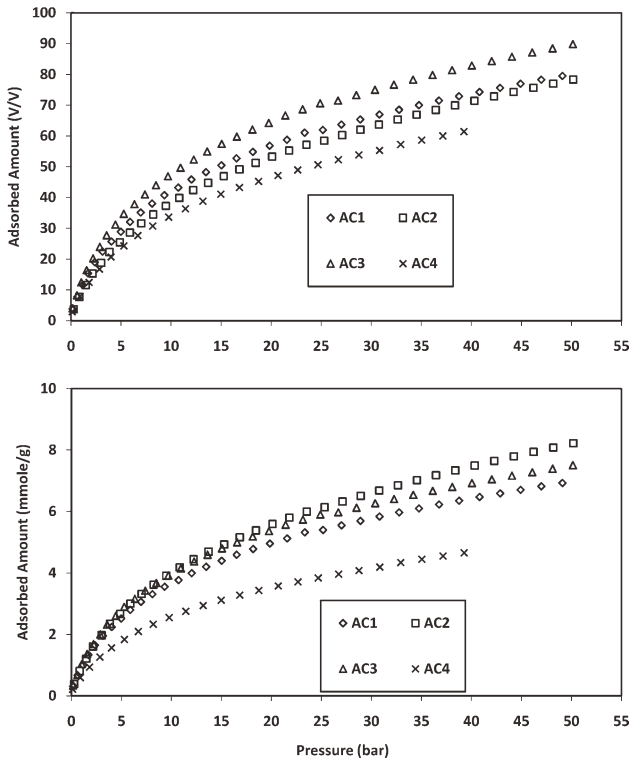

Figure 3. Volume to volume base comparison of the adsorption capacity among the four granular activated carbons. Mass to mass base comparison of the adsorption capacity among the four granular activated carbons.

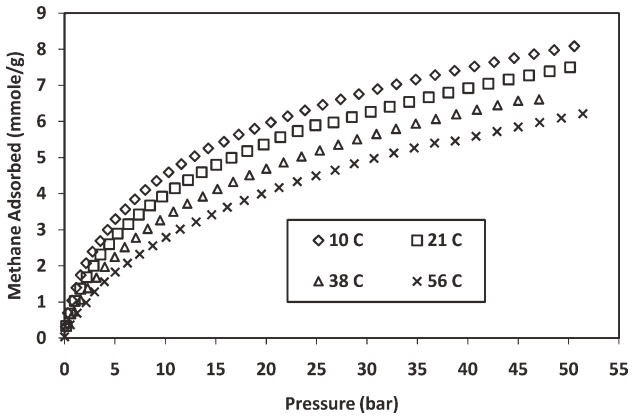

Figure 4. Comparison of methane adsorbed amount at different temperatures for AC3.

AC3 has the lowest average pore width of 17.47 Å among the four granular activated carbons as calculated by Barret-Joyner-Halenda(BJH) method (Table 1). The average pore width increases in the order of AC3(17.47 Å) < AC1(18.00 Å) < AC2(18.70 Å) < AC4(20.64 Å). Earlier theoretical studies[23–25] found that for methane adsorption on slit-pore activated carbon, the optimum pore width is 11.2–11.4 Å to create the maximum density for the adsorbed phase. Since the pore width of AC3 is close to the optimum pore width, it has the higher adsorption density, which contributes to AC3's highest volume to volume capacity for methane adsorption.

Since AC3 performs better than the others on volume to volume based comparison for methane adsorption, in the remaining part of the article, the data for AC3 will be used in the discussion and modeling. Figure 4 shows the temperature effect on methane adsorption on AC3. It is clear that the higher the adsorption temperature, the lower amount of methane adsorbed. This is due to the fact that adsorption is exothermic. According to the Le Chatelier's principle, the endothermic desorption will be favored when temperature increases. Therefore, less amount of methane is adsorbed at higher temperatures.

To calculate the stored amount of methane inside the adsorber vessel, the amount of the methane compressed inside the mesopores, macropores and the space among granular activated carbon particles is added to the liquid-like adsorbed phase inside micropores. Figure 5 compares the methane stored for ANG and CNG at various pressures at 21°C. At about 50 bars, the adsorber packed with AC3 can adsorb and store 90 and 120 times the volume of the adsorber cell, respectively. The same adsorber packed with AC3 only requires a pressure of about 10 bars to store the same amount of methane by compression at 50 bars. So, the advantage of adsorbed methane storage is obvious.

Empirical Modeling

Many semiempirical approaches have been proposed and they are quite successful in describing equilibrium data.[26] These isotherm equations include Freundlich, Sips, Toth and Unilan equations. The Freundlich isotherm equation is not valid at the low- and high- end of the pressure range because it does not give proper Henry law behavior at low-pressure,[27] and does not have a finite limit when the pressure is sufficiently high. It is generally valid in the narrow range of the adsorption data. Although the Sips equation addresses the problem of Freundlich equation of continuing increase of the adsorbed amount with an increase in pressure, it does not have a proper Henry law behavior at low-pressure. However, Toth isotherm equation satisfies both the low- and high-end requirement and describes many systems with submonolayer coverage very well. Unilan isotherm equation (uniform distribution and Langmuir local isotherm) assumes that the energy distribution is uniform and local Langmuir isotherm is applied.

Here, methane adsorption on AC3 was modeled with temperature-dependent form of Sips, Toth and Unilan equations. The equations and their optimized parameters are listed in Table 2. Nonlinear least-square method is used to fit the experimental data and in-house developed MATLAB program is used to drive the MATLAB optimization toolbox solver lsqcurvefit. The average relative error for each method is also listed in Table 2. The average relative error is defined in Eq. 4

$$Average\ relative\ error\ (ARE)\% = \frac{\sum\left|\frac{Y_i^{\exp} - Y_i^{modeled}}{Y_i^{\exp}}\right|}{N} \qquad (4)$$

where N is the number of experimental data points, superscripts *exp* and *modeled* stand for the experimental and modeled values, respectively, Y represents the amount of methane adsorbed.

In Table 2, the n_0, t and s in the Sips, Toth and Unilan equations characterize the heterogeneity of the methane-granular activated carbon system; C_μ,$C_{\mu s}$,$C_{\mu s0}$ are adsorbed amount, saturation adsorbed amount and saturation adsorption amount at the reference temperature; b,b_0,$\bar{b}$, are adsorption affinity constant, adsorption affinity constant at reference temperature and adsorption affinity constant at average adsorption energy, R is gas constant, P is adsorption pressure x,α, P are parameters, and Q is heat of adsorption. Q for Sips and Toth equations are quite different from each other. This should not cause any problem because Q in the Sips equation is the isosteric heat of adsorption at a

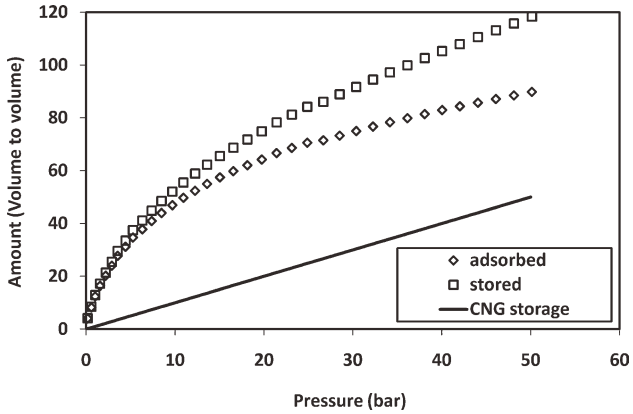

Figure 5. Amount of adsorbed and stored methane for AC3.

Table 2. Isotherm Equations Used to Model the Experimental Data and their Optimized Parameters

Equation Name	Equation Expression	Optimized Parameters using 294.15 K as reference temperature	ARE (%)
Sips	$C_\mu = C_{\mu s}\frac{(bP)^{1/n}}{1+(bP)^{1/n}}$ $b = b_0 \exp\left[\frac{Q}{RT_0}\left(\frac{T_0}{T}-1\right)\right]$ $\frac{1}{n} = \frac{1}{n_0}+\alpha\left(1-\frac{T_0}{T}\right)$ $C_{\mu s} = C_{\mu s,0} exp\left[z\left(1-\frac{T}{T_0}\right)\right]$	$C_{\mu s,0} = 10.794\ mmole/g$ $\chi = 0$ $b_0 = 0.023753\ bar^{-1}$ $Q = 10.516\ kJ/mole$ $n_0 = 1.6512$ $\alpha = 0.64163$	1.7563
Toth	$C_\mu = C_{\mu s}\frac{bP}{[1+(bP)^t]^{1/t}}$ $b = b_0 exp\left[\frac{Q}{RT_0}\left(\frac{T_0}{T}-1\right)\right]$ $t = t_D+\alpha\left(1-\frac{T_0}{T}\right)$ $C_{\mu s} = C_{\mu s,0} exp\left[\chi\left(1-\frac{T}{T_0}\right)\right]$	$C_{\mu s,0} = 17.934\ mmole/g$ $\chi = 0$ $b_0 = 0.12929\ bar^{-1}$ $Q = 20.259\ kJ/mole$ $t_0 = 0.42718$ $\alpha = 0.2573$	1.3047
Unilan	$C_\mu = C_{\mu s} ln\left(\frac{1+\bar{b}e^{s}P}{1+\bar{b}e^{-s}P}\right)$ $\bar{b} = b_0 exp\left[-\frac{\bar{E}}{RT_0}\left(1-\frac{T_0}{T}\right)\right]$ $\bar{E} = \frac{E_{max}+E_{min}}{2}$ $s = \frac{E_{max}-E_{min}}{2RT}$ $C_{\mu s} = C_{\mu s,0} exp\left[\chi\left(1-\frac{T}{T_0}\right)\right]$	$C_{\mu s,0} = 28.115\ mmole/g$ $\chi = 0$ $b_0 = 0.001025\ bar^{-1}$ $\bar{E} = 15.803\ kJ/mole$ $s = 6.1961$ $E_{max} = 30.956\ kJ/mole$ $E_{min} = 0.6505\ kJ/mole$	2.9886

fractional loading of 0.5, while Q in the Toth equation is the isosteric heat of adsorption at zero fractional loading. The values of n_0, t and s in Table 2 all indicate the heterogeneity of the methane-granular activated carbon system.[26] As indicated in Table 2, Toth equation gives the highest accuracy in fitting the experimental adsorption data. Figure 6 shows that the optimized temperature-dependent Toth equation fits experimental data well in all the pressure range at different temperatures.

Isosteric Heat of Adsorption

The knowledge of the adsorption equilibrium and isosteric heat of adsorption is essential for proper design and operation of any gas-phase adsorption process. The isosteric heat of adsorption is usually estimated from the temperature dependence of the adsorption isotherm.[19,28,29] As discussed in the Experimental results section, the optimized Toth equation gives the best result in fitting experimental data. Here, this equation is used to calculate the isosteric heat of adsorption. Using Clausius-Clapeyron equation (Eq. 5), the equation for isosteric heat of adsorption is derived from the Toth equation as shown in Eq. 6

$$-\Delta H = RT^2\left(\partial \ln P/\partial T\right)_\theta \tag{5}$$

$$\begin{aligned}-\Delta H &= Q-\frac{1}{t}(\alpha RT_O)\left\{\ln(bP)-\left[1+(bP)^t\right]\ln\left|\frac{bP}{\left(1+(bP)^t\right)^{1/t}}\right|\right\}\\ &= Q-\frac{1}{t}(\alpha RT_O)\left\{\ln\left[\frac{\theta}{\left(1-\theta^t\right)^{1/t}}\right]-\frac{\ln\theta}{(1+\theta^t)}\right\}\\ &= Q-\frac{1}{t}(\alpha RT_0)\left\{\ln\left[\frac{C_\mu}{\left(C_{\mu s}^t-C_\mu^t\right)^{1/t}}-\frac{\ln\left(C_\mu/C_{\mu s}\right)}{\left(1-\left(C_\mu/C_{\mu s}\right)^t\right)}\right]\right\}\end{aligned} \tag{6}$$

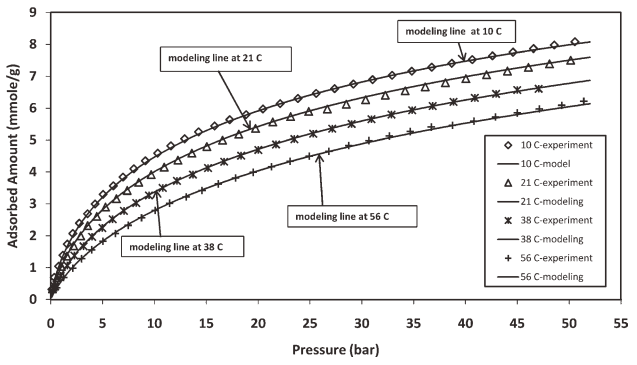

Figure 6. Modeling and experimental data for AC3 at different temperatures.

The isosteric heat of adsorption (Eq. 6) is a function of loading of adsorbates or pressure. Now, the meaning of Q in Eq. 6 is clear; it is the isosteric heat when the fractional loading is zero. Figure 7 shows the variation of the isosteric heat of adsorption for AC3 with loading at four different temperatures. The value of isosteric heat of adsorption determined by Eq. 6 for AC3 is close to those reported values of 20 KJ/mol in the literature.[30] The decrease of the isosteric heat with loading physically means that methane molecules prefer to adsorb onto the sites of high-energy. Then, as adsorption progresses methane molecules adsorb onto the sites of low-energy, which results in a slow increase in the amount of adsorbed vs. pressure. This finding is also in agreement with the slope of adsorption isotherm as indicated in Figure 6.

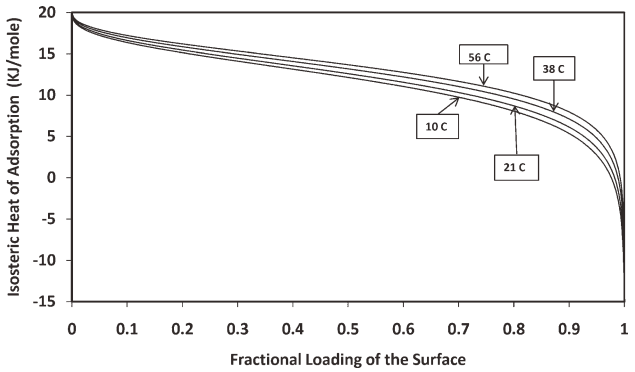

Figure 7. Calculated isosteric heat of adsorption for AC3 vs. loading using the Toth equation.

Integral Heat of Adsorption

Equation 6 can be numerically integrated to get the integral heat of adsorption,[31] which is the total amount of heat of adsorption released during the adsorption process. Therefore, the following procedure can be developed to estimate the integral heat of adsorption, which needs to be removed from an adsorber bed to control the bed temperature constant during adsorption process:

(a) Experimental measurement of adsorption isotherms at different temperatures.

(b) Use experimental data to optimize the parameters of the temperature-dependent Toth equation parameters.

(c) Use Toth equation to predict the amount of adsorption at a certain temperature and pressure.

(d) Integrate isosteric heat of adsorption curve to get the integral heat of adsorption—the total amount of isosteric heat of adsorption up to a certain pressure at a certain temperature.

Using the aforementioned procedure and assuming a constant bed temperature, the integral heat of adsorption heat released is calculated for an adsorber packed with 1 kg of AC3 at a temperature range of 10–60°C, and a pressure range of 0–50 bars. Although Figure 7 shows that isosteric heat is slightly higher at higher adsorption temperature, Figure 8 shows the integral heat of adsorption released at higher temperature is less than that at lower temperature. This is because of the less amount of methane adsorbed at higher temperature.

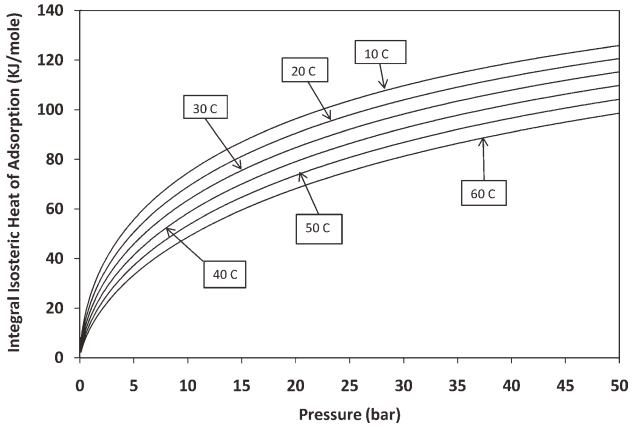

Figure 8. Integral heat of adsorption for methane adsorption process.

Conclusions

The detailed analysis of high-pressure methane adsorption and storage results at the temperature and pressure range of 10–56°C, and 0–50 bars has allowed us to draw the following conclusions.

Physical characteristics of granular activated carbon such as BET surface area, micropore volume, packing density and pore-size distribution all play important role in determining the amount of methane adsorbed.

Isosteric heat of adsorption of methane on granular activated carbons increases with temperature and decreases with loading, which indicates the heterogeneity of the methane-granular activated carbon system.

A procedure is developed to calculate the integral heat of adsorption in the adsorption process. The integral heat of adsorption increases with decrease of adsorption temperature. The higher amount of adsorption can account for this even though a slight lower isosteric heat of adsorption at lower adsorption temperature. This procedure can be used to predict the integral heat of adsorption released in the isothermal adsorption process and it is important information for the design and operation of an industrial adsorber.

Literature Cited

1. Cook TL, Komodromos C, Quinn DF, Ragan S. *Adsorbent storage for natural gas vehicles*. In: Burchell TD. *Carbon Materials for Advanced Technologies*. Oxford: Elsevier Science, Ltd; 1999:269–302.
2. Lu X-C, Li F-C, Ted, WA. Adsorption measurement in Devonian shales. *Fuel*. 1995;74:599–603.
3. Chang KJ, Talu O. Behavior and performance of adsorptive natural gas storage cylinders during discharge. *Appl Therm Eng*. 1996;16: 359–374.
4. Inomata K, Kanatawa K, Urabe Y, Hosono H, Araki T. Natural gas storage in activated carbon pellets without a binder. *Carbon*. 2002; 40:87–93.
5. Wegrzyn J, Gurevich M. Adsorbent storage of natural gas. *Appl Energy*. 1996;55:71–83.
6. Goetz V, Biloé S. Efficient dynamic charge and discharge of an adsorbed natural gas storage system. *Chem Eng Comm*. 2005;192: 876–896.
7. Menon VC, Komarneni S, Porous adsorbents for vehicular natural gas storage: a review. *J Porous Mater*. 1998;5:43–58.
8. Biloé S, Goetz V, Mauran S. Dynamic discharge and performance of a new adsorbent for natural gas storage. *AIChE J*. 2001;47:2819–2830.
9. Basumatary R, Dutta P, Prasad M, Srinivasan K. Thermal modeling of activated carbon based adsorptive natural gas storage system. *Carbon*. 2005;43:541–549.
10. Celzard A, Fierro V. Preparing a suitable material designed for methane storage: a comprehensive report. *Energy Fuels*. 2005;19: 573–583.
11. Pfeifer P, Ehrburger-Dolle F, Rieker TP, Gonzalez MT, Hoffman WP, Molina-Sabio M, Rodriguez-Reinoso F, Schumidt PW, Voss DJ. Nearly space-filling fractal networks of carbon nanopores. *Phys Rev Lett*. 2002;88:115502–1–115502–4.
12. Shao X, Wang W, Zhang X. Experimental measurements and computer simulation of methane adsorption on activated carbon fibers. *Carbon*. 2007;45:188–195.
13. Seki K. Design of an adsorbent with an ideal pore structure for methane adsorption using metal complexes. *Chem Commun*. 2001; 16:1496–1497.

14. Eddaoudi M, Kim J, Rosi N, Vodak D, Wachter J, O'Keeffe M, Yaghi OM. Systematic design of pore size and functionality in isoreticular mofs and their application in methane storage. *Science*. 2002;295:469–472.
15. Dűren T, Sarkisov L, Yaghi OM, Snurr RQ. Design of new materials for methane storage. *Langmuir*. 2004;20:2683–2689.
16. Ma S, Sun D, Simmons JM, Collier CD, Yuan D, Zhou H-C. Metal-Organic framework from an anthracene derivative containing nanoscopic cages exhibiting high methane uptake. *J Am Chem Soc*. 2008;130:1012–1016.
17. Atwood J L, Barbour LJ, Jerga A. Storage of methane and Freon by interstitial van der Waals confinement. *Science*. 2003;296:2367–2369.
18. Harlick PJE, Tezel FH. Adsorption of carbon dioxide, methane and nitrogen: Pure and binary mixture adsorption by ZSM-5 with SiO_2/Al_2O_3 ratio of 30. *Sep Sci Technol*. 2002;37:33–60.
19. Li P, Tezel FH. Adsorption Separation of N_2, O_2, CO_2, and CH_4 Gases by β-Zeolite. *Microporous Mesoporous Mater*. 2007;98:94–101.
20. Li P, Tezel FH. Pure and binary adsorption equilibria of carbon dioxide and nitrogen on silicalite. *J Chem Eng Data*. 2008;53:2479–2487.
21. Gumma S, Talu O. Gibbs dividing surface and helium adsorption. *Adsorption*. 2003;9:17–28.
22. Salehi E, Taghikhani V, Ghotbi C, Lay EN, Shojaei A. Theoretical and experimental study on the adsorption and desorption of methane by granular activated carbon at 25°C. *J Natural Gas Chem*. 2007;16:415–422.
23. Tan Z, Gubbins KE. Adsorption in carbon micropores at supercritical temperatures. *J Phy Chem*. 1990;94:6061–6069.
24. Matranga KR, Myers AL, Glandt ED. Storage of natural gas by adsorption on activated carbon. *Chem Eng Sci*. 1992;47:1569–1579.
25. Chen X S, McEnaney B, Mays TJ, Alcaniz-Monge J, Cazorla-Amoros D, Linares-Solano A. Theoretical and experimental studies of methane adsorption on microporous carbons. *Carbon*. 1997;35:1251–1258.
26. Do DD. *Adsorption Analysis: Equilibria and Kinetics, Series in Chemical Engineering*. London, UK: Imperial College Press; 1998.
27. Talu O, Myers AL. Rigorous thermodynamic treatment of gas adsorption. *AIChE J*. 1988;34:1887–1893.
28. Hacskaylo JJ, LeVan DM. Correlation of adsorption equilibrium data using a modified Antoine equation: a new approach for pore-filling models. *Langmuir*. 1985;1:97–100.
29. Sundaram N, Yang RT. Isosteric heats of adsorption from gas mixtures. *J Colloids Interface Sci*. 1998;198:378–388.
30. Esteves IAAC, Lopes, MSS, Nunes PMC, Mota JPB. Adsorption of natural gas and biogas components on activated carbon. *Sep Purif Technol*. 2008;62:281–296.
31. Myers AL. Thermodynamics of adsorption in porous materials. *AIChE J*. 2002;48:145–160.

Manuscript received Oct. 24, 2010, and revision received Feb. 21, 2011.